Available online at www.sciencedirect.com
SCIENCE DIRECT®
Thermochimica Acta 401 (2003) 159–168
thermochimica acta
www.elsevier.com/locate/tca

A new method for the determination of the unfrozen matrix concentration and the maximal freeze-concentration

Jens Liesebach [a,*], Thomas Rades [b], Miang Lim [a]

[a] *Department of Food Science, University of Otago, P.O. Box 56, Dunedin, New Zealand*
[b] *School of Pharmacy, University of Otago, Dunedin, New Zealand*

Received 11 October 2002; accepted 12 November 2002

Abstract

During the freezing process, water is partially separated as ice and the solutes are concentrated in the unfrozen matrix (UFM). With further lowering of the temperature, the UFM becomes highly viscous. The high viscosity of the UFM prolongs ice formation and makes it difficult to accurately determine the glass transition (T_g') and the concentration (C_g') of the maximally freeze-concentrated matrix. In this study, a new method for the determination of the concentration of the UFM was developed using differential scanning calorimetry (DSC). Sugar solutions were frozen, annealed at temperatures slightly above the expected T_g', rapidly cooled and then heated to 20 °C. The UFM concentrations of the annealed samples were obtained by estimating the solute concentration corresponding to the T_g at the respective annealing temperature. The dependence of the T_g on experimental conditions such as the annealing time, annealing temperature and cooling rate was studied in detail. Values for C_g' and T_g' were obtained by linear and quadratic extrapolations of the experimental data over a short temperature and solute concentration range. The maximal freeze-concentrations of glucose, sucrose and maltose were determined to be 79.9, 80.9 and 80.3% (w/w), respectively. Results of this study were in good agreement to previously published data.

Keywords: Maximal freeze-concentration; Glass transition; DSC; Phase diagram; Sugar

1. Introduction

Freezing is commonly used to stabilize food products. During the freezing process, water is partially separated as ice and solutes are concentrated among the ice formed. The solutes and the unfrozen water are referred to as the unfrozen matrix (UFM). A state diagram of a glucose matrix is shown in Fig. 1. The upper curve is referred to as the ice melting curve (T_m), but may be more accurately called a solubility curve for ice in the solute solution [1]. The lower curve is referred to as the glass transition curve (T_g), which is the transition between a viscous rubbery state and an extremely viscous glassy state. In the glassy state the mobility of components decreases and therefore, the rate of the diffusion limited reactions decreases [2,3].

At the temperature (T_g'), where the T_m curve and the T_g curve intersect, maximal freeze-concentration (C_g') is achieved [4]. When the solute concentration is close to C_g', the viscosity of the system increases dramatically. The high viscosity delays the formation of ice and thus inhibits maximal freeze-concentration [5]. Generally, sugar solutions with a solute concentration above 70% do not form ice, but rather go from the rubbery state straight into the glassy state [5–7]. The delay in ice formation makes it difficult to determine the physical properties of the system as it is in a

* Corresponding author. Fax: +64-3-179-7567.
E-mail address: jens_liesebach@gmx.de (J. Liesebach).

0040-6031/03/$ – see front matter © 2002 Elsevier Science B.V. All rights reserved.
PII: S0040-6031(02)00546-4

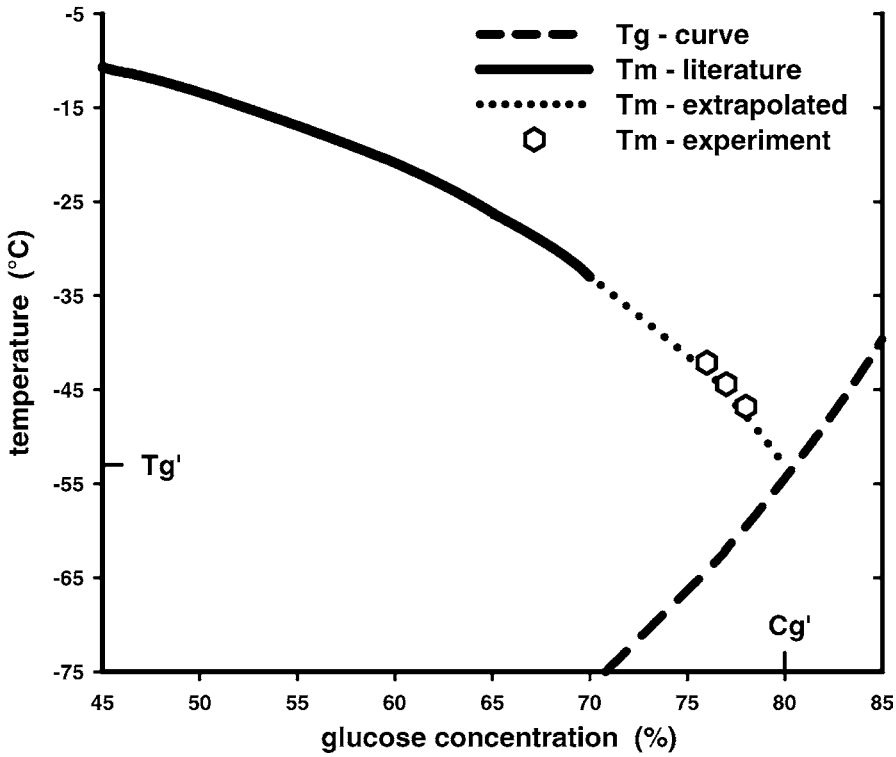

Fig. 1. State diagram of glucose, where the T_g curve was generated from values in this experiment and the T_m curve was generated from [18].

thermodynamically metastable state. However, the T_g' of the system can be determined by extrapolating the melting temperatures towards the T_g curve [8]. The accuracy of this extrapolated T_g' depends greatly on the accuracy of the lowest measured T_m and the distance between the lowest measured T_m and the T_g curve, because the T_m curve is not linear but follows a function of higher order. The lower the temperature, the steeper the gradient of the T_m curve (Fig. 1).

Several methods have been used to study the phase behavior of frozen systems, such as differential scanning calorimetry (DSC), nuclear magnetic resonance (NMR) [9] and dynamic mechanical thermal analysis (DMTA) [10]. In the DSC, the heating scan of a frozen sugar solution exhibits two transitions near the T_g'. The first transition (at the lower temperature) is called T_{r1} and the second transition (at the higher temperature) is called T_{r2} [11]. The T_{r1} has been shown to be the T_g of the UFM [6]. The glass transition of the UFM occurs over a temperature range and coincides with a dramatic change of viscosity, which can promote devitrification and ice formation. However, these changes are more likely in matrices of low UFM concentrations and may lead to a superimposed enthalpy change over the DSC trace of a glass transition.

Two methods have commonly been employed to determine the C_g' using DSC. In the first method, the area under the heat flow curve was used to calculate the amount of ice in the sample [12,13]. The accuracy of this method relies on the limits of the integral and the values for the temperature dependent specific heat and latent heat of the components [14]. In the second method, the samples are stored at various temperatures in order to achieve maximal freeze-concentration. After annealing these samples are cooled below the T_g of the UFM. The T_g' and C_g' is then determined from the T_{r1} of the following heating scan [6,15]. Temperature modulated DSC (TMDSC) of an aqueous sucrose matrix showed that kinetically limited ice crystallization still takes place when annealed at temperatures near T_{r1} after 5 h, however, when annealed at temperatures near T_{r2} very little ice

formation was observed in the same time frame [16]. Therefore, the C'_g of the latter method depends on both the annealing temperature and annealing time. Since the samples were only annealed for one fixed time interval, it is likely that annealing for a longer time would influence the concentration of the UFM as reactions are kinetically restricted in this area [17].

In this study, a novel approach was used to determine the UFM concentration below the lowest previously recorded T_m, e.g. for glucose the lowest T_m was −30 °C [18] (Fig. 1) and for sucrose it was −19 °C [19]. The C'_g and T'_g values can then be predicted by extrapolation of the data since the data points are close to the T_g curve. The sugar solution is frozen and then annealed at a temperature above the T'_g. Once the quasi-equilibrium is reached no further ice is formed or melted, thus the concentration of the UFM remains constant. The sample is then rapidly cooled below the T_g of the UFM and in a subsequent heating scan the T_g of the UFM is measured. Upon lowering the temperature, the frozen sample can form more ice. However, if the cooling rate is sufficiently fast, further ice formation can be inhibited. For each sugar investigated in this experiment, the optimal conditions in the DSC were determined.

2. Materials and methods

2.1. Sample preparation

Sugar solutions were prepared using anhydrous glucose (Analar grade, BDH, Poole, UK), maltose monohydrate (GPR grade, BDH, Poole, UK), sucrose (Analar grade, BDH, Poole, UK) and double distilled water. Solutions of low sugar concentrations were made by dissolving the sugar at room temperature or in a temperature controlled water bath at 65 °C. The concentration of the solution was determined from its weight after dissolution. High solute concentrations were prepared by pipetting a 66% (w/w) solution into pre-weighed DSC pans. The solutions were then dried in a desiccator and the solute concentration of each solution was calculated from the loss of weight. After the T_g determination, the samples were observed under a microscope to ensure the absence of sugar crystals. The results from solutions containing crystals were disregarded. The T_g of pure sugars was determined from freeze-dried 10% (w/w) solutions, which were stored over phosphorous pentoxide (P_2O_5) for 8 days. Samples (17.2±3.8 mg) were placed into pre-weighed aluminum pans (24.44 ± 0.01 mg) and hermetically sealed. The weights of the DSC pans were measured using an electronic ultramicro balance.

2.2. Thermal analysis

2.2.1. Calibration and T_g analysis

DSC studies were carried out on a Pyris 1 (Perkin-Elmer) equipped with a liquid nitrogen cooling unit. The DSC was calibrated with water (HPLC grade, 99.999%, Aldrich) and cyclohexane (HPLC grade 99.94%, Aldrich) at a scanning rate of 5 K/min. The thermograms were analyzed using Pyris 3.6 software (Perkin-Elmer). The T_g was determined as the midpoint of the change in the specific heat capacity of the lower transition (T_{r1}) after baseline subtraction. To determine the T_g, two tangents were added to the thermogram. The tangent below the transition was aligned to the heat flow. The tangent above the transition was set at the highest point of the transition and aligned to a parallel fit to the first tangent (Fig. 6).

2.2.2. Determination of T_g curve of non-frozen sugar solutions

Samples of known solute concentrations were cooled to at least 30 K below the expected T_g. These samples were then heated at a rate of 5 K/min. From the T_g of these solutions a T_g curve was generated using Eq. (1)

$$T_g \frac{xT_{r1} + z(100 - x)T_{r2}}{x + z(100 - x)} \quad (1)$$

where T_g is the glass transition temperatures of the aqueous sugar samples, T_{r1} and T_{r2} the glass transition temperatures of each component, x the weight fraction of the sugar and z is the value for the curvature of the trendline. The values for T_g were obtained from solute concentrations ranging from 62 to 100% (w/w). The values for T_{r1}, T_{r2} and z were free parameters for the fit as this trendline was used as a calibration curve for the data obtained from the DSC experiment in this study. The best fit for the curve was obtained by calculating the minimum sum of squares of the difference between the experimental and T_g values from Eq. (1).

2.2.3. Effect of annealing time on T_g

The sugar solutions were fast frozen to −100 °C, and then heated to annealing temperatures above the expected T_g' values [17]. After defined time intervals (5–180 min), the samples were cooled to approximately 25 K below the expected T_g at a nominal cooling rate of 220 K/min, then reheated to the previous annealing temperature at a heating rate of 5 K/min. The last two steps were repeated until the total annealing time was 180 min. Each time the sample was heated, the T_g was determined.

2.2.4. Effect of cooling rate on T_g of annealed samples

The samples were fast frozen to −100 °C, then heated to the annealing temperature. After annealing for 60 min, the samples were cooled at different nominal cooling rates (100–220 K/min) to approximately 25 K below the expected T_g, then heated to 20 °C at a heating rate of 5 °K/min. The T_g was determined from the last heating scan.

2.2.5. Determination of the sugar concentration in the UFM

The sugar samples were fast frozen to −100 °C, then heated to the lowest temperature from the optimal annealing temperature range and annealed for 60 min. After annealing, the samples were cooled to approximately 25 K below of the expected T_g at a nominal cooling rate of 220 K/min, then heated to the next highest annealing temperature at a scanning rate of 5 K/min. This procedure was repeated until the last annealing temperature was reached. Each time the sample was heated, the T_g was determined. The UFM concentration for samples annealed at various temperatures was obtained from the T_g curve by estimating the solute concentration corresponding to the T_g at the respective annealing temperature.

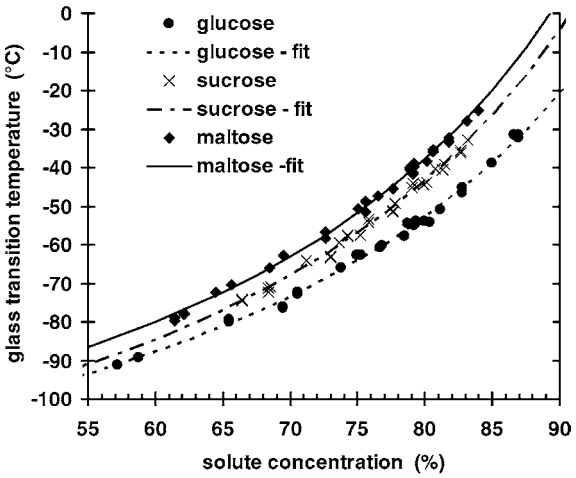

Fig. 2. Glass transition temperatures of various sugars as a function of solute concentration. Lines indicate the T_g curves generated using Eq. (1) with T_{r1}, T_{r2} and z as free parameters for the fit.

3. Results and discussion

3.1. T_g of sugar solutions

The T_g curves of glucose, maltose and sucrose were generated using Eq. (1) and are shown in Fig. 2. The T_g values for the pure sugars are summarized in Table 1 and were in excellent agreement with previous results. In the literature, a T_g value of −131 °C (midpoint) is commonly referred to as the T_g of water [20]. The extrapolated T_g of amorphous water for each system was slightly higher than the literature value. This might be related to the extrapolation over a 60% solute concentration range and free setting of the parameters T_{r1}, T_{r2} and z in Eq. (1). Free settings of parameters was used to obtain the best fit for the experimental results.

Table 1
T_g values from the fitted curve

Sugar	T_g for sugar (°C)		T_g for water (°C)	
	Fit	Literature	Fit	Literature
Glucose	35	31 [22], 37 [23], 38 [24], 39 [25]	−126	−131 [20], −137 [26]
Sucrose	68	57 [25], 62 [21], 70 [24]	−128	−131 [20], −137 [26]
Maltose	85	87 [21], 91 [23], 95 [24]	−123	−131 [20], −137 [26]

3.2. Optimization of method

The method for the determination of the UFM concentration near the T_g' was optimized for each of the sugars studied. In the following sections, only results of the optimization procedure for glucose are shown. However, similar evaluations were carried out for sucrose and maltose samples.

The influence of the annealing time on the T_g of the sample was studied by measuring the T_g at different time intervals and annealing temperatures. The total annealing time at each annealing temperature was 180 min. The differences between the T_g after different annealing times $\times$ ($x < 180$ min) and the T_g at 180 min are illustrated in Fig. 3. The T_g is closely related to the solute concentration in the UFM, which could explain the observed trends. The T_g values of samples annealed above $-45\,^{\circ}$C decreased over time, which could have been caused by the dilution of the UFM through the melting of ice. On the other hand, samples annealed at $-45\,^{\circ}$C and below increased their T_g values over time, which could be a result of further ice formation.

At different annealing temperatures the time needed for the system to equilibrate was different. In this study, it was assumed that a quasi-equilibrium between the ice and UFM was reached when the difference between the T_g of an annealed sample and the T_g of the sample that had been annealed for 180 min was less than 0.2 K. Therefore, samples annealed at -46, -45 and $-42\,^{\circ}$C reached quasi-equilibrium after 60 min, whereas samples annealed below $-46\,^{\circ}$C and above $-42\,^{\circ}$C needed more than 60 min to be in quasi-equilibrium. Based on these results, the optimal annealing temperatures for an annealing time of 60 min were between -46 and $-42\,^{\circ}$C.

The effect of the cooling rate on the T_g was determined at different annealing temperatures. The difference between the T_g at various cooling rates and the T_g at the maximum nominal cooling rate of 220 K/min is shown in Fig. 4. The cooling rate at an annealing temperature of $-30\,^{\circ}$C had a strong influence on the T_g, whereas samples annealed at temperatures closer to T_g' were less affected. In this study, it was assumed that the T_g was unaffected by the cooling rate when the difference between the T_g determined at a nominal

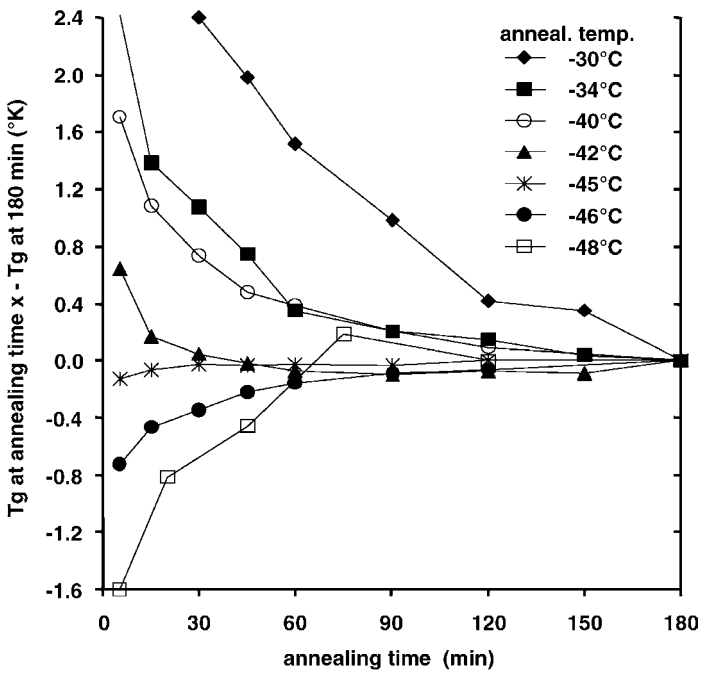

Fig. 3. Effect of annealing time on the T_g of a 54% glucose solution for different annealing temperatures.

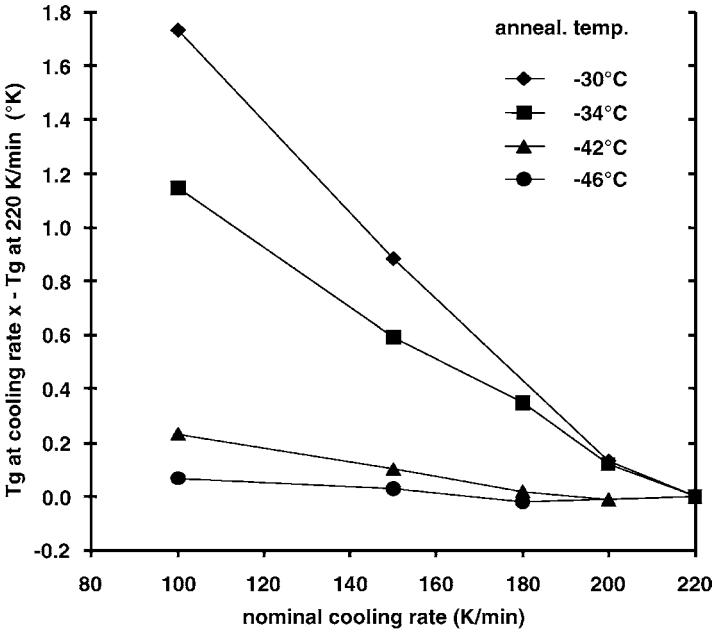

Fig. 4. Effect of cooling rate on the T_g of a 54% glucose solution at different annealing temperatures.

cooling rate of 150 K/min and the T_g at the maximum cooling rate of 220 K/min was less than 0.2 K. At annealing temperatures below −42 °C the differences in the T_g at nominal cooling rates from 150 to 220 K/min were less than 0.2 K. Therefore, a nominal cooling rate of 220 K/min appeared to be sufficient for accurate T_g determination at annealing temperatures below −42 °C.

The very high cooling rates stated above are nominal cooling rates based on the program settings of the DSC, not the actual cooling rates. The cooling rate in the sample holder is dependent on factors such as the temperature difference between the sample and cooling medium, sample size and thermal conductivity. At the start of each cooling step, the sample was held at the annealing temperature for about 1 s and then the temperature decreased sharply (Fig. 5). Since the DSC requires time to reach a fast cooling rate, the nominal cooling rates are considered as cooling drives. For example, a nominal cooling rate of 220 K/min lowered the sample temperature by about 20 K in the first 8 s. This means that the cooling rate in the sample holder was on average 150 K/min in the first 8 s. However, each nominal cooling rate achieves a different sample cooling rate, therefore the nominal cooling rates represent different sample cooling rates.

3.3. Determination of glucose concentration in the UFM

The above measurements yielded the optimal settings for the determination of the UFM concentration. The nominal cooling rate was set at 220 K/min and annealing temperatures were between −46 and −42 °C for a period of 60 min. The heating curves of the 59% glucose sample after annealing at −46 to −42 °C are shown in Fig. 6 and summarized in Fig. 7. At higher annealing temperatures the T_g of the glucose samples decreased. The slopes of the T_g values versus the annealing temperature plots for different initial concentrations were similar, however, there was a variability of ±1 K for the T_g at the same annealing temperature for different initial glucose concentrations. This variability might be related to different sample positions in the DSC sample holder or differences in sample size.

The T_g of the UFM followed the predicted trend, that is, as the annealing temperature increased, the T_g

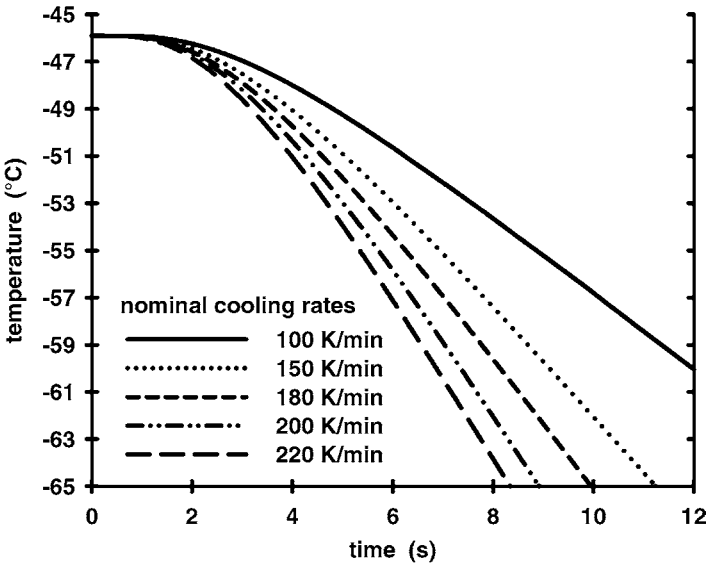

Fig. 5. Analysis of the sample cooling rate of a 54% glucose solution at an annealing temperature of −46 °C.

and the UFM concentration of the annealed sample decreased. The UFM concentration for samples annealed at various temperatures was obtained from the fitted T_g curve by estimating the solute concentration corresponding to the T_g at the respective annealing temperature (Fig. 7). At solute concentrations of 75–80% (w/w), a change in the T_g by 1 K corresponds to a change of approximately 0.5% in solute concentration. The UFM concentrations for each annealing temperature are recorded in Table 2. The solute concentration at the annealing temperature were extrapolated towards the T_g curve to determine the C'_g and T'_g. The results of the linear and quadratic extrapolation are illustrated in Fig. 8 and summarized

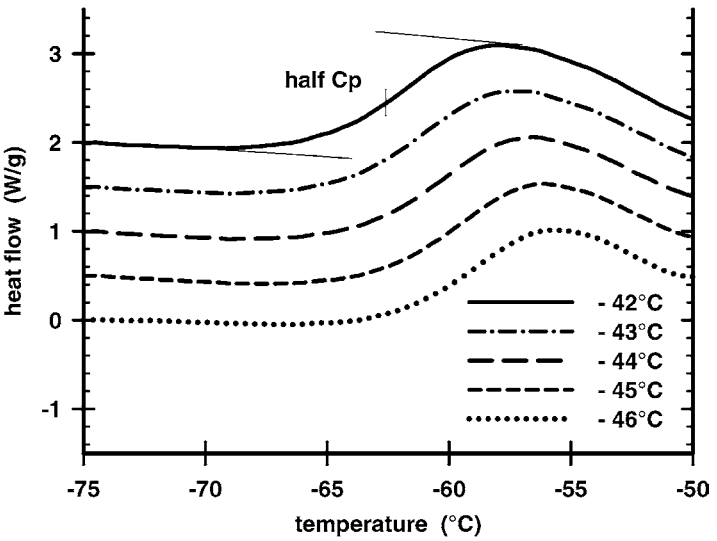

Fig. 6. T_g analysis of a heating scan of a 59% glucose solution after annealing at −46 to −42 °C.

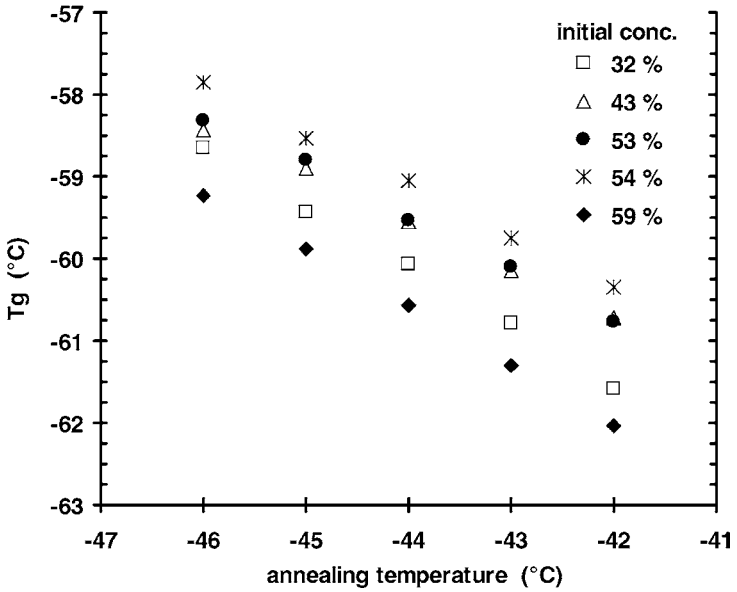

Fig. 7. T_g values of the annealed samples with various initial glucose concentrations.

Table 2
UFM concentrations for glucose, sucrose and maltose

Annealing temperature (°C)	Glucose (%, w/w)	Annealing temperature (°C)	Sucrose (%, w/w)	Maltose (%, w/w)
		−34	78.8 ± 0.2	
−46	77.7 ± 0.3	−33	78.5 ± 0.2	
−45	77.4 ± 0.3	−32	78.1 ± 0.2	78.5 ± 0.1
−44	77.1 ± 0.2	−31	77.8 ± 0.2	78.2 ± 0.1
−43	76.8 ± 0.2	−30	77.5 ± 0.2	77.9 ± 0.2
−42	76.5 ± 0.2	−29		77.5 ± 0.2
		−28		77.2 ± 0.2

in Table 3. The type of extrapolation used had little influence on the values of C'_g and T'_g since the UFM concentrations obtained were close to the maximal freeze-concentration. For this reason, it appears justifiable to determine the C'_g and T'_g as the point of intersection between the T_g curve and the linear extrapolation of the T_m values. A curvature towards lower values is expected (Fig. 1, T_m curve) as the melting temperature depends on the initial concentration. In this study, each quadratic extrapolation had a curvature towards lower temperatures and fulfills the expectations for a melting curve (Fig. 8).

3.4. Determination of sucrose and maltose concentrations in the UFM

The optimal annealing temperatures for sucrose and maltose were −34 to −30 and −32 to −28 °C, respectively. Interestingly, for all three sugars the lowest annealing temperature for an annealing time of 60 min was identical to the T_{r2} values from Roos [21]. The T_{r2} has been referred to as the onset of ice melting

Table 3
C'_g and T'_g values for glucose, sucrose and maltose

Type of extrapolation	Glucose		Sucrose		Maltose	
	T'_g (°C)	C'_g (%)	T'_g (°C)	C'_g (%)	T'_g (°C)	C'_g (%)
Linear	−53.1 ± 0.3	79.9 ± 0.1	−40.8 ± 0.3	80.9 ± 0.1	−37.1 ± 0.2	80.3 ± 0.1
Quadratic	−53.9 ± 0.4	79.6 ± 0.2	−40.9 ± 0.4	80.7 ± 0.3	−37.1 ± 0.3	80.2 ± 0.1

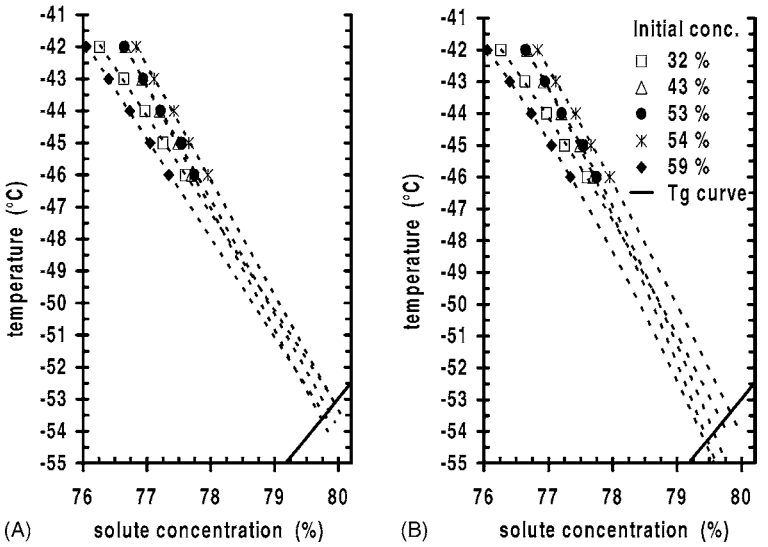

Fig. 8. Linear (A) and quadratic (B) extrapolation of the determined glucose concentrations towards the experimentally determined T_g curve.

[17], where the UFM becomes less concentrated at this and higher temperatures. A decrease in the UFM concentration causes a decrease in viscosity, which allows the molecules to move more freely. This may explain why the quasi-equilibrium was reached in a shorter time frame. The solute concentrations of the UFM at various annealing temperatures are listed in Table 2. The C'_g and T'_g values from both the linear and quadratic extrapolation are summarized in Table 3. Again, the type of extrapolation did not significantly change the C'_g and T'_g values of the sugar systems (Table 3), due to the close distance between the quasi-equilibrated UFM and T_g curve. Therefore, linear extrapolation was also used to determine the C'_g and T'_g of sucrose and maltose.

The results of this study were similar to previously published results that used T_{r1} to determine C'_g and T'_g values, however, the C'_g results from the area under the peak method are distinctively lower (Table 4). This may be due to the use of constant values for the latent heat of ice and specific heat of the solutes [14]. Furthermore, T_{r2} was considered to be the T_g of the

Table 4
Published T'_g and C'_g values for glucose, sucrose and maltose

Method	Glucose		Sucrose		Maltose		Reference
	T'_g (°C)	C'_g (%)	T'_g (°C)	C'_g (%)	T'_g (°C)	C'_g (%)	
DSC[a]	−43	70.9	−32	64.1	−29.5	80.0	[12]
DSC[a]	−42.4	74.6			−29.7	76.7	[13]
DSC[b]			−32	83.0			[27]
DSC[c]			−40	81.2			[6]
DSC[c]	−53	80.0	−41	81.7	−37	81.6	[17]
DMTA	−52.0	80.7	−39.4	82.6	−34.0	82.8	[10]

[a] Area under the curve was used to determine C'_g and T_{r2} was considered as the T'_g of the UFM.
[b] Comparison of the T_{r2} with the T_g of vitrified samples.
[c] Samples were annealed to achieve C'_g and T_{r1} was considered as the T'_g of the UFM.

UFM [12,13]. The higher onset temperature for the integration reduces the area under the heat flow curve and thus results in a smaller UFM concentration. The T_g' values obtained by DMTA are close to the values of this study [10]. This suggests that T_{r1} can be used to determine the T_g values of the UFM and the UFM concentrations. Interferences from superimposed transitions at the T_{r1}, such as ice formation, are therefore likely to be negligible.

The new method developed in this study determines the C_g' and T_g' of the UFM and also describes the shape of the melting curve. Furthermore, the annealing times are shortened to 60 min. The results of this study should now be adapted to more complex systems. By extending the annealing time or increasing the cooling rates the accuracy of the method will be further increased. A longer annealing time than used in this study would allow the system to reach quasi-equilibrium at temperatures closer to T_g'. Higher cooling rates would inhibit ice formation when samples are cooled from higher annealing temperatures. In both cases the data range for the extrapolation would be extended.

4. Conclusion

A novel approach for the determination of the solute concentration in the UFM was developed. This method does not aim to reach the maximal freeze-concentration since the system is kinetically restricted at C_g'. Instead, this method aims to determine the quasi-equilibrium of the UFM concentration at temperatures near the maximal freeze-concentration. Since the data obtained are close to the T_g curve, a linear extrapolation of the UFM concentrations values towards lower temperatures was used to determine C_g' and T_g' of glucose, sucrose and maltose. The results are in agreement with previously reported data based on methods with long annealing times. This study can be used to obtain accurate values for the UFM concentration, C_g' and T_g' with shorter annealing times.

References

[1] S. Ablett, A. Clark, M. Izzard, P. Lillford, J. Chem. Soc., Faraday Trans. 88 (1992) 8.
[2] M.H. Lim, D.S. Reid, in: H. Levine, L. Slade (Eds.), Water Relationships in Foods, vol. 302, Plenum Press, New York, 1991, p. 103.
[3] N.C. Brake, O.R. Fennema, J. Food Sci. 64 (1999) 25.
[4] F. Franks, Water—A Comprehensive Treatise, Plenum Press, New York, 1985.
[5] H.D. Goff, M.E. Sahagian, Thermochim. Acta 280 (1996) 449.
[6] S. Ablett, M.J. Izzard, P.J. Lillford, J. Chem. Soc., Faraday Trans. 88 (1992) 789.
[7] S. Ablett, M.J. Izzard, P.J. Lillford, I. Arvanitoyannis, J.M.V. Blanshard, Carbohydr. Res. 246 (1993) 13.
[8] I. Arvanitoyannis, J.M.V. Blanshard, S. Ablett, M.J. Izzard, P.J. Lillford, J. Sci. Food Agric. 63 (1993) 177.
[9] S. Ablett, A. Darke, M.J. Izzard, P. Lillford, in: J.M.V. Blanshard, P.J. Lillford (Eds.), The Glassy State in Foods, Nottingham University Press, Nottingham, 1993, p. 207.
[10] I.B. Cruz, J.C. Oliveira, W.M. MacInnes, Int. J. Food Sci. Technol. 36 (2001) 539.
[11] M.E. Sahagian, H.D. Goff, Thermochim. Acta 246 (1994) 271.
[12] H. Levine, L. Slade, J. Chem. Soc., Faraday Trans. 1 84 (1988) 2619.
[13] T.W. Schenz, K. Courtney, B. Israel, Cryo.-Lett. 14 (1993) 91.
[14] D.S. Reid, J. Hsu, W. Kerr, in: J.M.V. Blanshard (Ed.), The Glassy State in Foods, Nottingham University Press, Nottingham, 1993, p. 123.
[15] Y. Roos, M. Karel, Cryo.-Lett. 12 (1991) 367.
[16] S.A. Knopp, S. Chongprasert, S.L. Nail, J. Thermal Anal. Calorimetry 54 (1998) 659.
[17] Y.H. Roos, J. Thermal Anal. 48 (1997) 535.
[18] F.E. Young, J. Phys. Chem. 61 (1957) 616.
[19] F.E. Young, F.T. Jones, J. Phys. Coll. Chem. 53 (1949) 1334.
[20] G.P. Johari, A. Hallbrucker, E. Mayer, Nature (London) 330 (1987) 552.
[21] Y.H. Roos, Carbohydr. Res. 238 (1993) 39.
[22] A.L. Ollett, R. Parker, J. Texture Stud. 21 (1990) 355.
[23] P.D. Orford, R. Parker, S.G. Ring, A.C. Smith, Int. J. Biol. Macromol. 11 (1989) 91.
[24] P.D. Orford, R. Parker, S.G. Ring, Carbohydr. Res. 196 (1990) 11.
[25] L. Finegold, F. Franks, R.H.M. Hatley, J. Chem. Soc., Faraday Trans. 1 85 (1989) 2945.
[26] E. Mayer, J. Mol. Struct. 250 (1991) 403.
[27] R.H.M. Hatley, C. van den Berg, F. Franks, Cryo.-Lett. 12 (1991) 113.